

# 000 SMOOTHED-MODERNBERT: CO-ATTENTIONAL SYN- 001 ERGY OF PROBABILISTIC TOPIC MODELS AND MOD- 002 ERNBERT THROUGH DYNAMIC FUSION 003 004

005 **Anonymous authors**  
006  
007 Paper under double-blind review  
008  
009  
010  
011

## ABSTRACT

013 Document classification remains a critical challenge in natural language processing  
014 (NLP) as text volumes and thematic complexity escalate. Although transformer-  
015 based architectures like BERT excel at capturing contextual semantics, they of-  
016 ten overlook the latent thematic structures inherent in document-level discourse.  
017 Conversely, probabilistic topic models effectively distill coarse-grained thematic  
018 patterns but struggle with nuanced contextual dependencies. To address these lim-  
019 itations, this study introduces a novel hybrid approach that synergizes the contextual  
020 depth of ModernBERT with the interpretable thematic representations of smoothed-  
021 Dirichlet-based topic models. Our model aligns token-level representations with  
022 document-level thematic distributions by optimizing contextual and topic objec-  
023 tives through a co-attention mechanism layer. By utilizing a dynamic fusion layer,  
024 where co-attention scores dynamically gate and blend BERT’s embeddings with  
025 topic mixtures at each instance, the approach captures both fine-grained context and  
026 global theme interplay in a unified representation. Our method bridges a critical gap  
027 in the NLP methodology, paving the way for enhanced model generalizability in do-  
028 mains that require both thematic abstraction and contextual granularity. Empirical  
029 evaluations on benchmark corpora demonstrate consistent classification robustness  
030 over standalone approaches. To ensure the reproducibility of our experiments and  
031 encourage further research, we open-source our implementation code.

## 1 INTRODUCTION

032 Document classification is a fundamental task in natural language processing (NLP), which underpins  
033 applications such as news categorization, sentiment analysis, and information retrieval Devlin et al.  
034 (2019); Bao et al. (2019). Early methods relied on hand-crafted features and statistical models,  
035 but the exponential growth in text volume and complexity has driven a shift toward deep learning.  
036 Recurrent architectures such as LSTMs Clavié et al. (2021) and GRUs Ravanelli et al. (2018); Ahmed  
037 et al. (2023); Mortezapour Shiri et al. (2023) automated feature extraction and sequential patterns  
038 captured, although their inherently sequential nature limits parallelism and long-range dependency  
039 modeling Nam et al. (2017). Hybrid approaches that combine truncated attention with recurrent units  
040 or integrate self-attention into bidirectional GRUs have partially alleviated these issues Nam et al.  
041 (2017); Sun et al. (2019b); Jiang & Wang (2022).

042 The advent of transformers, particularly BERT with its multi-head self-attention and contextual  
043 embeddings Vaswani et al. (2017), has further transformed the field by allowing full parallel pro-  
044 cessing of entire sequences. Fine-tuning techniques have delivered state-of-the-art results across  
045 benchmarks Sun et al. (2019a); Wang et al. (2020a), and extensions combining BERT with capsule  
046 networks Wang et al. (2020b); Liu et al. (2012) or graph neural networks Li & Jia (2025); Qasim et al.  
047 (2022); Jamshidi et al. (2024); Davidson & Dym (2024) continue to push performance. Despite these  
048 advances, transformer models can overlook global thematic coherence, misread sarcasm or broader  
049 discourse, and offer limited interpretability. In contrast, probabilistic topic models Luo et al. (2022),  
050 such as smoothed Dirichlet distribution, identify coherent themes but struggle with contextual nuance  
051 Nallapati et al. (2007). Bridging this gap, hybrid frameworks like TopicBERT fuse Gaussian topic  
052 priors with BERT embeddings Chaudhary et al. (2020a), yet typically employ shallow concatenation  
053 that underutilizes the complementary strengths of each paradigm.

Despite these advances, reconciling token-level contextual precision with document-level thematic interpretability remains an open challenge. To this end, we propose Smoothed-ModernBERT: co-attentional synergy of probabilistic topic models and ModernBERT through dynamic fusion (SD-MoBERT), a novel architecture that integrates ModernBERT with a dynamically smoothed Dirichlet topic model via a co-attentional synergy mechanism. Unlike prior shallow-fusion methods, our model jointly optimizes the dynamically fused contextual and thematic losses, fostering mutual reinforcement between granular semantics and global topics. We demonstrate that this integration yields better performance and interpretability across multiple benchmark corpora, bridging the methodological gap between contextual depth and thematic coherence. The main contributions of our studies are summarized as follows:

1. We propose a novel hybrid architecture that integrates ModernBERT’s contextual semantics with smoothed-Dirichlet topic modeling, bridging neural and probabilistic paradigms to jointly optimize fine-grained context and interpretable thematic structures.
2. Dynamic co-attention fusion: We introduce a gated mechanism that dynamically blends token-level BERT embeddings with smoothed Dirichlet document-level topic mixtures, enabling adaptive weighting of local and global thematic information.
3. Empirical Validation and Reproducibility: We show that SD-MoBERT consistently outperforms baseline models and make our full implementation publicly available to facilitate future research and practical adoption <https://github.com/anonymousPapersSubmissions/Smoothed-ModernBERT>.

The remainder of this paper is organized as follows. Section 2 reviews related work on transformer encoders and topic modeling. Section 3 reviews the background studies, while Section 4 presents the proposed model. The experimental results and conclusion are presented in Section 5 and Section 6, respectively.

## 2 RELATED WORK

Document classification has evolved through five key paradigms: traditional statistical methods, neural architectures, transformers, hybrid topic-neural frameworks, and co-attentional synergy. Early approaches relied on manually engineered features such as Bag-of-Words (BoW) Qader et al. (2019) and TF-IDF Christian et al. (2016), which quantified the importance of words, but ignored context. Bag-of-N-Grams Li et al. (2016) improved phrase representation, while bag-of-means models integrated word embeddings, although semantic nuances remained elusive.

Neural architectures addressed these limitations through character-level CNNs Zhang et al. (2015); Bielik et al. (2017), though fixed kernel sizes hindered long-range dependency modeling Yue et al. (2018). The compact CNN variants Talai & Kherici (2023) reduced parameters, but retained locality constraints. Sequential models such as LSTMs Clavié et al. (2021) and GRUs Michael et al. (2024) captured longer contexts but suffered from limited parallelism. Bidirectional GRUs with truncated drop loss Abbasi et al. (2024) mitigated class imbalance, yet sequential processing persisted as a bottleneck.

Transformers revolutionized the field via self-attention mechanisms Vaswani et al. (2017), with BERT Devlin et al. (2019) achieving state-of-the-art through bidirectional pre-training. ModernBERT Warner et al. (2024) scaled efficiency via flash attention but lacked document-level thematic coherence. Hybrid enhancements like capsule networks Wang et al. (2020b) and graph neural networks Li & Jia (2025) improved hierarchical features but struggled with global topic integration.

Hybrid topic-neural frameworks emerged to bridge thematic and contextual modeling. Probabilistic topic models (PTMs) Wang et al. (2022) like LDA Blei et al. (2003) abstracted themes but ignored word order. Neural topic models (NTMs) Wu et al. (2024); Ojo & Bouguila (2024) used variational autoencoders for continuous distributions, while Topic-BERT Chaudhary et al. (2020a) combined BERT with Gaussian topic vectors, a shallow fusion lacking synergy. Class-based TF-IDF clustering enhanced interpretability but limited classifier integration. Recent work includes SBERT-TM for short texts Cheng et al. (2023) and ensemble models like ENTM-TS Voskergian et al. (2024), though computational costs constrained scalability. Concurrently, co-attentional architectures Lee et al.

108 (2025) optimized feature fusion but overlooked probabilistic topic priors, leaving opportunities for  
 109 deeper integration of thematic structure and contextual semantics.  
 110

111 **2.1 MOTIVATION: TOWARD CO-ATTENTIONAL SYNERGY**  
 112

113 Co-attention mechanisms have proven effective in multimodal reasoning by aligning heterogeneous  
 114 representations Nam et al. (2017). However, their application to intra-textual fusion of context  
 115 and themes remains underexplored. SD-MoBERT diverges from shallow fusion by employing a  
 116 co-attention layer that dynamically aligns ModernBERT’s token embeddings with smoothed Dirichlet  
 117 topic distributions. This mutual reinforcement allows topic priors to guide attention heads toward  
 118 thematically salient tokens, while contextual features refine topic coherence via variational inference.  
 119 By unifying transformer efficiency, probabilistic topic modeling, and co-attentional interaction in a  
 120 single, scalable architecture, SD-MoBERT transcends the limitations of each paradigm and offers a  
 121 robust, informed solution for document classification in complex, heterogeneous corpora.  
 122

123 **3 BACKGROUND STUDIES**

124 **3.1 SMOOTHED DIRICHLET DISTRIBUTION (SD)**

125 The smoothed Dirichlet distribution extends the conventional Dirichlet distribution by introducing  
 126 regularization, making it a robust prior for categorical data in Bayesian frameworks. This adaptation  
 127 is particularly advantageous for mitigating zero-probability issues in sparse categorical settings, such  
 128 as emotion recognition in social media analytics Najar & Bouguila (2022), happiness modeling,  
 129 and pain estimation Najar & Bouguila (2021). By redistributing probability mass across categories,  
 130 smoothing enhances model stability Heckerman (1998) and generalizability Chen & Goodman (1999).  
 131 Following Nallapati et al. (2007), a smoothed proportion  $\mathbf{F}^s$  is derived from raw word counts using a  
 132 tunable parameter  $\lambda$ :

$$\mathbf{F}^s = \frac{\mathbf{X}^s - (1 - \lambda) \mathbf{X}^{GE}}{\lambda} \quad (1)$$

133 where  $\mathbf{X}^s$  and  $\mathbf{X}^{GE}$  denote the smoothed feature proportion and baseline word distribution (e.g.,  
 134 general English), respectively. The likelihood of observing  $\mathbf{X}^s$  under the smoothed Dirichlet prior is:  
 135

$$p(\mathbf{X} \mid \boldsymbol{\alpha}, \varepsilon) = \frac{1}{B(\boldsymbol{\alpha} + \varepsilon)} \prod_{i=1}^K X_i^{(\alpha_i + \varepsilon) - 1}, \quad \frac{1}{B(\boldsymbol{\alpha} + \varepsilon)} = \frac{\Gamma(\sum_i (\alpha_i + \varepsilon))}{\prod_i \Gamma(\alpha_i + \varepsilon)}, \quad (2)$$

136 where  $K$  and  $\varepsilon > 0$  denote the vocabulary size and smoothing parameter, respectively,  $X_i^s$  the  
 137 smoothed feature, and  $\alpha_i$  is the concentration parameters. The normalizer  $B(\vec{\alpha})$  ensures a valid  
 138 probability simplex.

139 In contrast to prior work that smooths raw inputs Nallapati et al. (2007), our method applies smoothing  
 140 directly to the Dirichlet parameters and the latent representation. Preliminary experiments revealed  
 141 that smoothing raw features induces covariate shifts in the feature representations, destabilizing  
 142 training. Thus, our approach maintains feature consistency while enabling end-to-end optimization.  
 143 This strategy aligns with the model’s dynamic adaptation capabilities.  
 144

145 **3.2 MODERNBERT**  
 146

147 ModernBERT builds upon BERT’s bidirectional Transformer architecture to deliver powerful context-  
 148 ual embeddings while addressing the original’s quadratic time and memory complexity in relation to  
 149 sequence length Warner et al. (2024). By extending its maximum input length from 512 to 8,192  
 150 tokens, ModernBERT can capture long-range dependencies and global context in lengthy documents.  
 151 A key innovation is FlashAttention, an optimized CUDA kernel that reorganizes attention computa-  
 152 tions to reduce memory accesses and fully exploit on-chip caches, yielding up to a two-fold speedup  
 153 in self-attention layers Dao et al. (2022). Positional information is encoded using rotary positional  
 154 embeddings (RoPE), which applies continuous rotation transformations to token representations  
 155 and scales gracefully to very long sequences without the need for learned positional parameters  
 156 Warner et al. (2024). To further mitigate computational costs, ModernBERT employs sequence  
 157 packing and blockwise attention, splitting inputs into contiguous chunks and restricting attention to  
 158

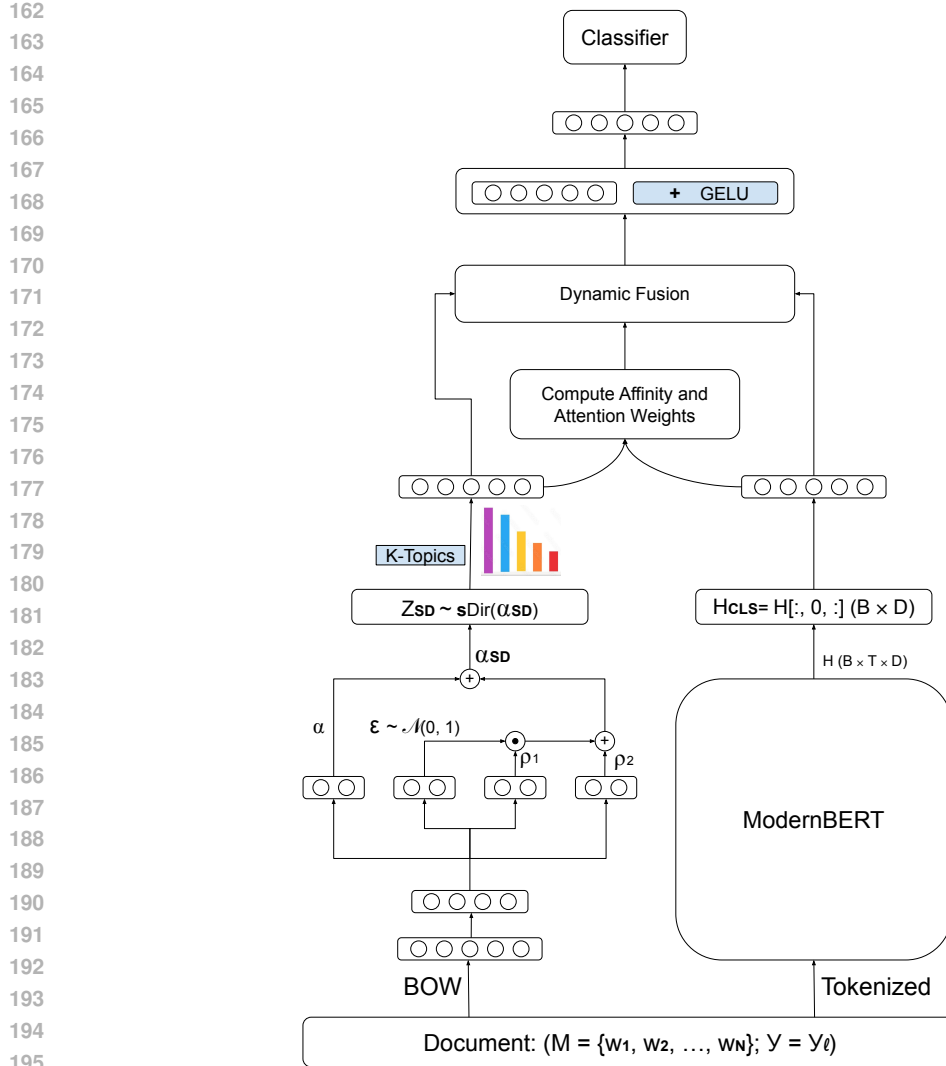


Figure 1: A schematic representation of the proposed SD-MoBERT model, leveraging smoothed Dirichlet neural topic model and ModernBERT.

intra-block and adjacent-block interactions; this achieves sub-quadratic complexity while preserving essential cross-chunk dependencies Warner et al. (2024). Finally, feed-forward sublayers incorporate low-rank matrix factorizations and sparse projection patterns that reduce parameter counts and confine expensive operations to the most informative tokens. These enhancements allow ModernBERT to handle long sequences of tokens efficiently, making it a scalable and context-rich foundation for hybrid models.

#### 4 PROPOSED MODEL: SMOOTHED-MODERNBERT (SD-MOBERT)

Figure 1 illustrates the architecture of SD-MoBERT, combining a neural topic model with an advanced transformer-based modernBERT. We employ ModernBERT because of its architectural innovations, such as support for up to 8,192 token contexts, FlashAttention, and rotary positional embeddings, which enable fast, memory-efficient processing of very long documents without sacrificing contextual depth Warner et al. (2024). Given a document  $M = \{w_1, w_2, \dots, w_N\}$  with label  $y$ , SD-MoBERT processes two parallel streams. Firstly, a normalized bag-of-words vector  $\mathbf{X} \in \mathbb{R}^V$  ( $V$  = vocabulary size) for latent topic inference is generated. Secondly, a copy of the document is segmented into

216 subword tokens  $\{t_n\}$  to generate a token sequence  $\{t_1, \dots, t_T\}$  ( $T \leq 8192$ ) via ModernBERT’s  
 217 tokenizer, producing contextual embeddings  $\mathbf{E} \in \mathbb{R}^{T \times D}$  (hidden size  $D$ ), with [CLS] and [SEP]  
 218 marking the start and the end.

219 In the generative process, we first draw from the neural topic model and infer a latent topic vector  
 220  $\mathbf{Z} \in \mathbb{R}^K$  ( $K$  topics) under a smoothed Dirichlet prior:  
 221

$$222 \quad \mathbf{Z}_{\text{SD}} \sim \text{sDir}(\boldsymbol{\alpha}_{\text{SD}}) \Leftarrow \frac{\exp(\boldsymbol{\alpha}_{\text{SD}}^i)}{\sum_{i=1}^K \exp(\boldsymbol{\alpha}_{\text{SD}}^i)} \quad (3)$$

$$223$$

$$224$$

$$225 \quad \boldsymbol{\alpha}_{\text{SD}} = \boldsymbol{\alpha} + \boldsymbol{\rho}_2 + \boldsymbol{\epsilon} \odot \exp(\log \boldsymbol{\rho}_1) \in \mathbb{R}^K, \quad (4)$$

$$226$$

227 where  $\boldsymbol{\alpha}$ ,  $\boldsymbol{\rho}_1$ , and  $\boldsymbol{\rho}_2$  are the neural topic model’s outputs,  $\boldsymbol{\epsilon} \sim \mathcal{N}(\mathbf{0}, \mathbf{I})$ .  
 228

229 Conversely, let the ModernBERT output be denoted by  $\mathbf{h}_{\text{CLS}}$ . We then project  $\mathbf{Z}_{\text{SD}}$  and  $\mathbf{h}_{\text{CLS}}$  each  
 230 through a linear layer followed by a GELU activation to produce  $\mathbf{Z}_{\text{SD}}^t$  and  $\mathbf{Z}_{\text{CLS}}$ , respectively. Next,  
 231 we define the attention score  $\mathbf{S}$  and the attention weight  $\mathbf{Z}_{\text{att}}$  as:

$$232 \quad \mathbf{S} = \langle \mathbf{Z}_{\text{SD}}^t, \mathbf{Z}_{\text{CLS}} \rangle_D + \mathbf{b}_0, \quad \mathbf{Z}_{\text{att}} = \sigma(\mathbf{S}) \quad (5)$$

$$233$$

234 where  $\mathbf{b}_0$  and  $\sigma$  denote the attention bias weight and sigmoid function, respectively. Following this,  
 235 we dynamically fuse representation as:

$$236 \quad \mathbf{Z}_{\text{fused}} = \mathbf{Z}_{\text{att}} \mathbf{Z}_{\text{SD}}^t + (1 - \mathbf{Z}_{\text{att}}) \mathbf{Z}_{\text{CLS}}, \quad \mathbf{Z} = \tanh(\mathbf{Z}_{\text{fused}}) \in \mathbb{R}^{B \times D} \quad (6)$$

$$237$$

238 where  $\mathbf{Z}$ ,  $B$  and  $D$  denote the latent representation, batch size, and sequence dimension, respectively.  
 239 The latent representation is further projected through two linear layers and fed to the classifier, and  
 240 we optimized with the joint loss:

$$241 \quad \mathcal{L} = \underbrace{- \sum_i y_i \log \hat{y}_i}_{\mathcal{L}_{\text{CE}}} + \beta \underbrace{\text{D}_{\text{KL}}(q(\mathbf{Z} | \mathbf{X}) \parallel \text{sDir}(\boldsymbol{\alpha}_{\text{SD}}))}_{\mathcal{L}_{\text{KL}}}, \quad (7)$$

$$242$$

$$243$$

$$244$$

245 where  $\beta$  balances classification accuracy against topic coherence and  $\mathcal{L}_{\text{CE}}$  denotes the classification  
 246 loss.  $y_i$  and  $\hat{y}$  represent the actual label and the prediction, respectively.  $\mathcal{L}_{\text{KL}}$  Ojo et al. (2025)  
 247 denotes the thematic loss that regularizes the latent space and penalizes the loss function to ensure  
 248 that the model does not overfit. By aligning the thematic representations from the Dirichlet-based  
 249 topic model with the contextual embeddings from ModernBERT through a co-attention mechanism,  
 250 SD-MoBERT achieves a synergistic understanding of documents. This fusion enables the model to  
 251 maintain interpretability through topic distributions while capturing nuanced contextual relationships,  
 252 improving the performance of document classification tasks. See Section B for more details on the  
 253 pseudocode for the generative process and Section B.1 for details on  $\mathcal{L}_{\text{KL}}$ .  
 254

## 255 5 EXPERIMENTAL RESULTS

### 256 5.1 EXPERIMENTAL SETTINGS

257 Please note that we conduct 30 separate experiments with different seeds using different validation  
 258 sets at each experiment. Thus, we report the average value of our experiments over 30 runs. We  
 259 explore the hyperparameter space using grid search to select the best combination of parameters for  
 260 the experiment. We use a learning rate of  $2e^{-5}$  with a warm-up of 10 and use AdamW optimizer,  
 261  $\beta = 0.2$ . We set the batch size and epoch to 8 and 20, respectively. We set the topic number of the  
 262 smoothed Dirichlet component to 100. Section C presents the effect of hyperparameter tuning.  
 263

### 264 5.2 DATASETS

265 We compare our proposed model with the baseline models on five widely used benchmark datasets,  
 266 allowing insightful comparisons. The 20 Newsgroups (20NG) dataset Albishre et al. (2015) comprises  
 267 18,846 documents distributed across 20 categories, ranging from sports and politics to technology  
 268 and religion. It contains 11,314 samples for training and 7,532 for testing. The Movie Review

(MR) dataset Haider Rizvi et al. (2025) contains 10,662 movie reviews balanced between 5,331 positives and 5,331 negatives for sentiment analysis. Ohsumed Haider Rizvi et al. (2025) consists of MEDLINE abstracts tagged in 23 categories of cardiovascular disease. It contains 7,400 documents, split into 3,357 for training and 4,043 for testing. Finally, we use the Reuters collection, drawn from the 1987 newswire, which is commonly evaluated via its R8 subset (8 classes, 5,485 training and 2,189 test documents) and R52 subset (52 classes, 6,532 training and 2,568 test documents) Moschitti & Basili (2004).

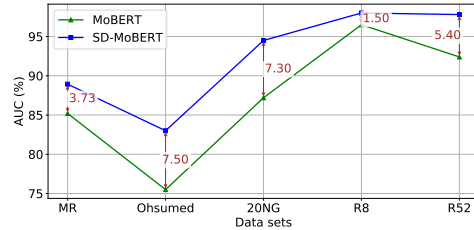
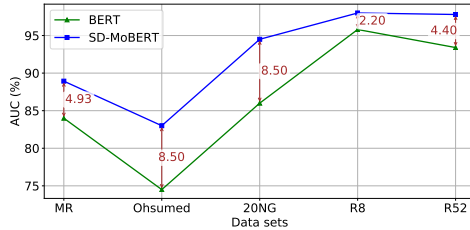


Figure 2: Analyses of the area under curve (AUC) of SD-MoBERT against BERT and MoBERT,  $K = 100$ ,  $\beta = 0.2$ .

### 5.3 BASELINE MODELS

To evaluate SD-MoBERT, we benchmark it against five close variants: BERT Devlin et al. (2019) and MoBERT Warner et al. (2024) without smoothed Dirichlet, SD-BERT (smoothed Dirichlet + BERT) Devlin et al. (2019), SD-RoBERTa (smoothed Dirichlet + RoBERTa-base) Masala et al. (2020), and SD-DistilBERT (smoothed Dirichlet + DistilBERT) Sanh et al. (2019), as well as a number of topic and graph-augmented models. These include TopicBERT-64/128 Chaudhary et al. (2020b), TextING Zhang et al. (2020), HyperGAT Ding et al. (2020), TextFCG Wang et al. (2023), TextSSL Piao et al. (2022), BertGCN Lin et al. (2021), GTC Liu et al. (2023), MHGAT Galke et al. (2022), and PaSIG-S Wang et al. (2025), providing a comprehensive backdrop for assessing the gains afforded by smoothed Dirichlet fusion in modern transformers.

### 5.4 AREA UNDER CURVE (AUC) ANALYSIS OF SD-MoBERT AGAINST BERT AND MoBERT

The AUC Çorbacıoğlu & Aksel (2023) plots the true positive rate (TPR) versus the false positive rate (FPR) to evaluate a model’s ability to differentiate between classes across different thresholds. We use the trapezoidal rule to approximate the AUC, defined in Yeh et al. (2002)

$$AUC \approx \sum_{i=1}^{n-1} (FPR_{i+1} - FPR_i) \cdot \frac{TPR_{i+1} + TPR_i}{2} \quad (8)$$

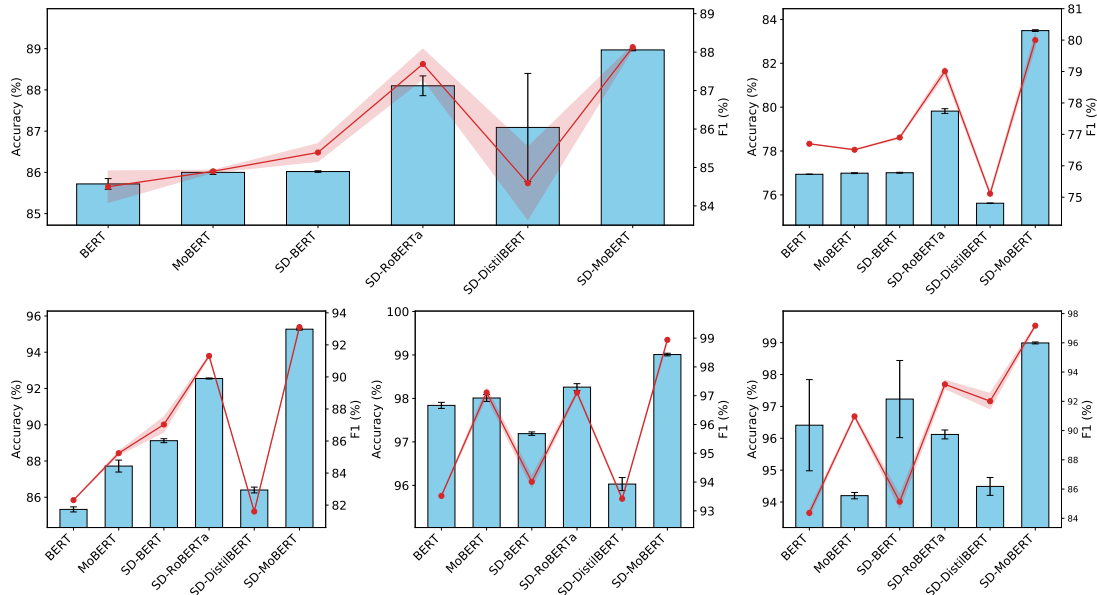
Figure 2a illustrates the relative AUC gains of SD-MoBERT over the original BERT encoder across the five datasets. SD-MoBERT (blue squares) consistently outperforms BERT (green triangles), with improvements ranging from 2.2% to 8.5%. The largest gains occur on the 20 Newsgroups and Ohsumed corpora (both 8.5% gains), while even on Reuters R8, the margin remains substantial at 2.2%. Similarly, Figure 2b shows the AUC improvements of SD-MoBERT’s relative to the MoBERT variant. Across all data sets, SD-MoBERT achieves gains between 1.5% on R8 and 7.5% on Ohsumed data sets. These results underscore the robustness of the smoothed Dirichlet in capturing the thematic structures inherent in document-level discourse and the dynamic fusion mechanism in enhancing discriminative power over the base ModernBERT architecture.

### 5.5 PERFORMANCE COMPARISON OF SD-MoBERT AGAINST BASELINES AND MODEL VARIANTS

Tables 1 and 2 present a detailed evaluation of SD-MoBERT relative to ten established baselines and five BERT-family variants across five benchmark datasets, reporting mean accuracy and F1

324  
 325 Table 1: Comparisons of the average test accuracy and F1 scores with their respective standard  
 326 deviations. We evaluate SD-MoBERT alongside other baseline models across three datasets (MR,  
 327 Ohsumed, and 20NG),  $K = 100$ ,  $\beta = 0.2$ .

328	329	Model	330 MR		331 Ohsumed		332 20NG	
			333 Accuracy	334 F1	335 Accuracy	336 F1	337 Accuracy	338 F1
330	331	TextING	79.75 $\pm$ 0.78	79.63 $\pm$ 0.85	73.51 $\pm$ 1.05	68.15 $\pm$ 0.77	85.13 $\pm$ 0.66	84.32 $\pm$ 0.12
		HyperGAT	76.64 $\pm$ 0.81	76.58 $\pm$ 0.92	66.55 $\pm$ 1.37	59.05 $\pm$ 1.84	83.29 $\pm$ 0.46	82.72 $\pm$ 0.24
		TextFCG	80.59 $\pm$ 0.29	80.56 $\pm$ 0.47	69.58 $\pm$ 0.39	56.16 $\pm$ 0.71	85.95 $\pm$ 0.33	84.91 $\pm$ 0.51
		TextSSL	75.74 $\pm$ 0.25	75.64 $\pm$ 0.38	62.01 $\pm$ 0.41	51.99 $\pm$ 0.78	79.55 $\pm$ 0.27	79.11 $\pm$ 0.65
		332 Baselines	TopicBERT-64	85.21 $\pm$ 0.91	85.01 $\pm$ 0.76	72.31 $\pm$ 0.33	71.13 $\pm$ 0.48	83.86 $\pm$ 0.55
			TopicBERT-128	86.89 $\pm$ 0.33	86.15 $\pm$ 0.64	74.10 $\pm$ 0.74	73.92 $\pm$ 0.22	82.60 $\pm$ 0.10
			BertGCN	84.92 $\pm$ 0.84	84.05 $\pm$ 0.67	71.88 $\pm$ 0.52	62.72 $\pm$ 0.47	88.69 $\pm$ 0.45
			GTC	77.22 $\pm$ 0.37	77.01 $\pm$ 0.24	69.72 $\pm$ 0.72	62.8 $\pm$ 0.11	87.03 $\pm$ 0.61
			MHGAT	78.09 $\pm$ 0.73	77.24 $\pm$ 0.57	72.88 $\pm$ 0.84	65.04 $\pm$ 1.60	92.68 $\pm$ 0.30
		333 Proposed Model Variants	PaSIG-S	87.05 $\pm$ 0.09	87.04 $\pm$ 0.09	81.18 $\pm$ 0.21	74.58 $\pm$ 0.42	93.21 $\pm$ 0.07
			BERT	85.72 $\pm$ 0.13	84.50 $\pm$ 0.41	76.94 $\pm$ 0.01	76.70 $\pm$ 0.00	85.33 $\pm$ 0.14
			MoBERT	86.00 $\pm$ 0.05	84.9 $\pm$ 0.03	76.99 $\pm$ 0.02	76.51 $\pm$ 0.01	87.72 $\pm$ 0.33
			SD-BERT	86.02 $\pm$ 0.02	85.39 $\pm$ 0.23	77.01 $\pm$ 0.02	76.90 $\pm$ 0.03	89.12 $\pm$ 0.11
			SD-RoBERTa	88.10 $\pm$ 0.24	87.69 $\pm$ 0.39	79.82 $\pm$ 0.11	79.01 $\pm$ 0.13	92.55 $\pm$ 0.03
			SD-DistilBERT	87.09 $\pm$ 1.31	84.59 $\pm$ 0.94	75.62 $\pm$ 0.01	75.11 $\pm$ 0.06	86.40 $\pm$ 0.16
			SD-MoBERT	<b>88.97 <math>\pm</math> 0.02</b>	<b>88.13 <math>\pm</math> 0.05</b>	<b>83.49 <math>\pm</math> 0.04</b>	<b>80.00 <math>\pm</math> 0.21</b>	<b>95.27 <math>\pm</math> 0.05</b>
								<b>93.11 <math>\pm</math> 0.07</b>



372  
 373 Figure 3: Comparison of the classification accuracy and F1 score in six transformer-based models  
 374 on five text classification benchmarks. The bar plots (sky blue) depict mean test accuracy with the  
 375 error bars, while the overlaid red lines trace mean F1 scores. Each subplot corresponds to a different  
 376 dataset: MR (top left), Ohsumed (top right), 20NG (bottom left), Reuters R8 (bottom center), and  
 377 Reuters R52 (bottom right),  $K = 100$ ,  $\beta = 0.2$ .

378  
379  
380  
381  
382  
383  
384  
385  
386  
387  
388

389 Table 2: Comparisons of the average test accuracy and F1 scores with their respective standard  
390 deviations. We evaluate SD-MoBERT alongside other baseline models across two datasets (R8 and  
391 R52),  $K = 100$ ,  $\beta = 0.2$ .

392	393	Model	R8		R52	
			394	Accuracy	F1	Accuracy
395	396	TextING	97.45 $\pm$ 0.70	95.94 $\pm$ 0.63	94.95 $\pm$ 0.95	76.71 $\pm$ 0.87
397	398	HyperGAT	96.43 $\pm$ 0.63	92.12 $\pm$ 1.51	94.24 $\pm$ 0.54	72.35 $\pm$ 1.83
399	400	TextFCG	97.53 $\pm$ 0.34	92.44 $\pm$ 0.21	95.64 $\pm$ 0.15	69.13 $\pm$ 0.28
401	402	TextSSL	97.31 $\pm$ 0.42	93.01 $\pm$ 0.33	93.97 $\pm$ 0.66	72.79 $\pm$ 1.41
403	Baselines	TopicBERT-64	93.01 $\pm$ 0.29	92.11 $\pm$ 0.63	72.89 $\pm$ 0.57	72.18 $\pm$ 0.98
404		TopicBERT-128	93.94 $\pm$ 0.22	92.83 $\pm$ 0.51	73.42 $\pm$ 0.37	72.84 $\pm$ 0.29
405		BertGCN	97.94 $\pm$ 0.73	94.60 $\pm$ 0.44	95.50 $\pm$ 0.44	52.30 $\pm$ 0.73
406		GTC	97.21 $\pm$ 0.85	93.73 $\pm$ 0.64	94.51 $\pm$ 0.97	94.52 $\pm$ 0.77
407		MHGAT	97.65 $\pm$ 0.47	93.09 $\pm$ 1.21	94.78 $\pm$ 0.37	76.74 $\pm$ 1.06
408		PaSIG-S	<b>99.02 <math>\pm</math> 0.04</b>	98.16 $\pm$ 0.12	98.34 $\pm$ 0.03	85.99 $\pm$ 1.52
409		PaSIG-S	<b>99.02 <math>\pm</math> 0.04</b>	98.16 $\pm$ 0.12	98.34 $\pm$ 0.03	85.99 $\pm$ 1.52
410	411	BERT	97.84 $\pm$ 0.07	93.52 $\pm$ 0.01	96.41 $\pm$ 1.43	84.37 $\pm$ 0.25
412	413	MoBERT	98.01 $\pm$ 0.08	97.11 $\pm$ 0.15	94.20 $\pm$ 0.10	90.97 $\pm$ 0.09
414	Proposed Model Variants	SD-BERT	97.19 $\pm$ 0.04	94.01 $\pm$ 0.20	97.23 $\pm$ 1.21	85.14 $\pm$ 0.47
415		SD-RoBERTa	98.26 $\pm$ 0.08	97.11 $\pm$ 0.05	96.12 $\pm$ 0.14	93.16 $\pm$ 0.28
416		SD-DistilBERT	96.03 $\pm$ 0.15	93.42 $\pm$ 0.03	94.49 $\pm$ 0.28	92.01 $\pm$ 0.53
417		SD-MoBERT	99.01 $\pm$ 0.03	<b>98.94 <math>\pm</math> 0.07</b>	<b>98.99 <math>\pm</math> 0.03</b>	<b>97.17 <math>\pm</math> 0.07</b>
418		SD-MoBERT	99.01 $\pm$ 0.03	<b>98.94 <math>\pm</math> 0.07</b>	<b>98.99 <math>\pm</math> 0.03</b>	<b>97.17 <math>\pm</math> 0.07</b>
419	420	SD-MoBERT	99.01 $\pm$ 0.03	<b>98.94 <math>\pm</math> 0.07</b>	<b>98.99 <math>\pm</math> 0.03</b>	<b>97.17 <math>\pm</math> 0.07</b>
421	422	SD-MoBERT	99.01 $\pm$ 0.03	<b>98.94 <math>\pm</math> 0.07</b>	<b>98.99 <math>\pm</math> 0.03</b>	<b>97.17 <math>\pm</math> 0.07</b>
423	424	SD-MoBERT	99.01 $\pm$ 0.03	<b>98.94 <math>\pm</math> 0.07</b>	<b>98.99 <math>\pm</math> 0.03</b>	<b>97.17 <math>\pm</math> 0.07</b>
425	426	SD-MoBERT	99.01 $\pm$ 0.03	<b>98.94 <math>\pm</math> 0.07</b>	<b>98.99 <math>\pm</math> 0.03</b>	<b>97.17 <math>\pm</math> 0.07</b>
427	428	SD-MoBERT	99.01 $\pm$ 0.03	<b>98.94 <math>\pm</math> 0.07</b>	<b>98.99 <math>\pm</math> 0.03</b>	<b>97.17 <math>\pm</math> 0.07</b>
429	430	SD-MoBERT	99.01 $\pm$ 0.03	<b>98.94 <math>\pm</math> 0.07</b>	<b>98.99 <math>\pm</math> 0.03</b>	<b>97.17 <math>\pm</math> 0.07</b>
431	432	SD-MoBERT	99.01 $\pm$ 0.03	<b>98.94 <math>\pm</math> 0.07</b>	<b>98.99 <math>\pm</math> 0.03</b>	<b>97.17 <math>\pm</math> 0.07</b>

432 scores with their corresponding standard deviations. On the MR short-text sentiment classification  
 433 task, PaSIG-S achieved an average accuracy of  $87.05\% \pm 0.09$  and F1 score of  $87.04\% \pm 0.09$ .  
 434 SD-MoBERT raises accuracy to  $88.97\% \pm 0.02$ , a  $(88.97 - 87.05)/87.05 \times 100 \approx 2.3\%$  relative  
 435 gain, and boosts F1 to  $88.13\% \pm 0.05$ , a  $\approx 1.3\%$  improvement in F1. On the Ohsuemed corpus, SD-  
 436 MoBERT attains  $83.49\% \pm 0.04$  accuracy, outperforming the best baseline (PaSIG-S:  $81.18\% \pm 0.21$ )  
 437 by  $2.85\%$ , and achieves an F1 score of  $80.00\% \pm 0.21$ , a  $7.26\%$  over PaSIG-S's  $74.58\% \pm 0.42$ . These  
 438 gains underscore SD-MoBERT's enhanced ability to disambiguate complex medical terminology  
 439 where graph-based methods (e.g. HyperGAT) exhibit lower F1 score. For the 20 Newsgroups (20NG),  
 440 SD-MoBERT reaches  $95.27\% \pm 0.05$  accuracy, a  $2.21\%$  improvement over PaSIG-S's  $93.21\% \pm 0.07$ ,  
 441 and records an F1 of  $93.11\% \pm 0.07$ , surpassing the next-best model (MHGAT:  $91.94\% \pm 0.13$ ) by  
 442  $1.27\%$ . SD-MoBERT shows its ability to distinguish semantically overlapping categories.  
 443

444 On R8, PaSIG-S achieves  $99.02\% \pm 0.04$  accuracy and  $98.16\% \pm 0.12$  F1, while SD-MoBERT records  
 445  $99.01\% \pm 0.03$  (a negligible  $-0.01\%$  change) and  $98.94\% \pm 0.07$ , corresponding to a  $\approx 0.8\%$  F1  
 446 improvement. On Reuters R52, SD-MoBERT yields an F1 score of  $97.17\% \pm 0.07$ , representing a  
 447  $12.98\%$  increase over PaSIG-S's  $85.99\% \pm 1.52$ . Such a substantial margin highlights its robustness  
 448 in hierarchical news classification, where error propagation across parent-child categories is a known  
 449 challenge. When compared to other BERT variants, SD-MoBERT consistently delivers further gains.  
 450 In the MR short-text sentiment benchmark, accuracy improves from BERT's  $85.72\% \pm 0.13$  and  
 451 MoBERT's  $86.00\% \pm 0.05$  to  $88.97\% \pm 0.02$ , corresponding to relative increases of  $3.25\%$  and  $2.97\%$ ,  
 452 respectively. On Reuters R8, SD-MoBERT's F1 score of  $98.94\% \pm 0.07$  exceeds SD-RoBERTa's  
 453  $97.11\% \pm 0.05$  by  $1.88\%$ , demonstrating the efficacy of smoothed-Dirichlet regularization. Against  
 454 SD-DistilBERT on Ohsuemed, SD-MoBERT's F1 advantage of  $6.51\%$  ( $80.00\%$  vs.  $75.11\%$ ) further  
 455 confirms that model compression without careful calibration can degrade performance on specialized  
 456 domains. Across all five datasets, SD-MoBERT exhibits minimal performance variance (standard  
 457 deviations between  $\pm 0.02$  and  $\pm 0.07$ ), in stark contrast to several baselines and variants (e.g. TextSSL  
 458 on Ohsuemed, GTC on R52, and SD-DistilBERT on MR), whose larger fluctuations signal instability.  
 459 This consistency is attributable to the smoothed-Dirichlet fusion's ability to regularize confidence  
 460 estimates and mitigate overfitting. As shown in Table 3, we evaluate whether the observed accuracy  
 461 gains of SD-MoBERT over the best baseline (PaSIG-S) are statistically significant. As indicated in  
 462 Table 3, all p-values ( $\ll 0.05$ ), uniformly reject  $H_0$ , while the CIs remain vanishingly narrow. See  
 463 more details in Section E.  
 464

$$H_0: \mu_{\text{SD-MoBERT}} = \mu_{\text{PaSIG-S}} \quad \text{vs.} \quad H_1: \mu_{\text{SD-MoBERT}} \neq \mu_{\text{PaSIG-S}} \quad (9)$$

## 465 5.6 ERROR-BAR ANALYSIS OF ACCURACY AND F1 ACROSS PROPOSED MODEL VARIANTS

466 Figure 3 presents the error bar across the five data sets. The accuracy bars exhibit consistently  
 467 narrow error margins, typically under  $0.5\%$ , indicating that each model's mean performance is  
 468 highly stable over repeated runs. Notably, the unsmoothed BERT and MoBERT backbones show  
 469 slightly wider accuracy-bar spreads (up to  $1.3\%$  on SD-DistilBERT's R52 result), whereas the  
 470 smoothed-Dirichlet variants (SD-BERT, SD-RoBERTa, SD-DistilBERT, SD-MoBERT) reduce that  
 471 variability to under  $0.3\%$ , reflecting more reliable convergence. In contrast, the F1 scores (red  
 472 lines) display larger error bands, ranging from virtually zero for MoBERT on MR up to  $0.94\%$   
 473 for SD-DistilBERT, highlighting that the precision-recall balance is intrinsically more sensitive in  
 474 the architectures. Importantly, SD-MoBERT not only attains the highest mean accuracy and F1 in  
 475 every data set but also maintains among the smallest F1-error spreads ( $\leq 0.07\%$ ), underscoring its  
 476 robustness in both overall correctness and class-balanced performance.  
 477

## 478 5.7 LIMITATIONS

479 SD-MoBERT requires manual selection of the topic count  $K$ , as too few topics yield overly broad  
 480 themes and too many produce fragmented noise, necessitating costly hyperparameter searches. The  
 481 added topic model and co-attention layer also incur extra parameters and runtime overhead, and  
 482 learned topics may not transfer across domains without retraining. Future work will explore adaptive  
 483 topic estimation and computation efficiency. See more discussion on the time complexity and runtime  
 484 cost in Section F.  
 485

486  
 487 Table 3: Statistical analyses of SD-MoBERT over 30 runs using different validation sets and the best  
 488 baseline model (PaSIG-S) accuracy. The bold values signify p-values that are below 0.05, CI and  $S$   
 489 denote the class interval, and standard deviation, respectively,  $K = 100$ ,  $\beta = 0.2$ .

		MR	Ohsumed	20NG	R8	R52
SD-MoBERT	Mean (F1)	88.13	80.00	93.11	98.94	97.17
	Variance	$8.54e^{-4}$	$2.57e^{-2}$	$1.37e^{-3}$	$1.51e^{-3}$	$1.53e^{-3}$
	$S$	0.029	0.160	0.037	0.039	0.039
	CI	[88.120 – 88.140]	[79.943 – 80.057]	[93.097 – 93.123]	[98.926 – 98.954]	[97.156 – 97.184]
Best baseline (PaSIG-S)	F1	87.04	74.58	92.91	98.16	85.99
p-value		<b><math>2.378e^{-47}</math></b>	<b><math>3.782e^{-46}</math></b>	<b><math>3.087e^{-23}</math></b>	<b><math>1.487e^{-39}</math></b>	<b><math>5.488e^{-73}</math></b>

## 501 6 CONCLUSION

502 This study addresses the critical challenge of document classification in NLP by harmonizing the  
 503 complementary strengths of transformer architectures and probabilistic topic modeling. While  
 504 ModernBERT captures nuanced contextual semantics and topic models distill interpretable thematic  
 505 structures, their isolated applications leave a methodological gap in handling both granular context and  
 506 global discourse. Our proposed framework bridges this divide through a novel co-attention mechanism  
 507 that dynamically fuses token-level BERT embeddings with document-level smoothed-Dirichlet topic  
 508 distributions, enabling joint optimization of contextual and thematic objectives. Empirical validation  
 509 across benchmark corpora demonstrates that this synergistic approach achieves superior classification  
 510 robustness, outperforming standalone models by effectively leveraging multi-granular semantic  
 511 signals. The dynamic gating mechanism ensures adaptive weighting of contextual and thematic  
 512 features, enhancing generalizability across domains requiring both precision and abstraction. By  
 513 open-sourcing our implementation, we invite the community to build upon this work, advancing  
 514 methodologies that unify local and global text representations. This contribution not only advances  
 515 document classification but also establishes a blueprint for integrating neural and probabilistic  
 516 paradigms in NLP, fostering models that balance interpretability with state-of-the-art performance.  
 517 Future work will explore adaptive topic number estimation and multi-head co-attention to model  
 518 richer interactions between topics and tokens.

## 520 REFERENCES

521 Asima Akber Abbasi, Aneela Zameer, and Muhammad Asif Zahoor Raja. An enhanced strategy  
 522 for minority class detection using bidirectional gru employing penalized cross-entropy and self-  
 523 attention mechanisms for imbalance network traffic. *The European Physical Journal Plus*, 139(6):  
 524 530, 2024.

525 Shams Forruque Ahmed, Md Sakib Bin Alam, Maruf Hassan, Mahtabin Rodela Rozbu, Taoseef  
 526 Ishtiak, Nazifa Rafa, M Mofijur, ABM Shawkat Ali, and Amir H Gandomi. Deep learning  
 527 modelling techniques: current progress, applications, advantages, and challenges. *Artificial  
 528 Intelligence Review*, 56(11):13521–13617, 2023.

529 Khaled Albishre, Mubarak Albathan, and Yuefeng Li. Effective 20 newsgroups dataset cleaning.  
 530 In *2015 IEEE/WIC/ACM International Conference on Web Intelligence and Intelligent Agent  
 531 Technology (WI-IAT)*, volume 3, pp. 98–101. IEEE, 2015.

532 Yujia Bao, Menghua Wu, Shiyu Chang, and Regina Barzilay. Few-shot text classification with  
 533 distributional signatures. *International Conference on Learning Representations paper*, 2019.

534 Pavol Bielik, Veselin Raychev, and Martin Vechev. Program synthesis for character level language  
 535 modeling. In *International conference on learning representations*, 2017.

536 David M Blei, Andrew Y Ng, and Michael I Jordan. Latent dirichlet allocation. *Journal of machine  
 537 Learning research*, 3(Jan):993–1022, 2003.

540 Yatin Chaudhary, Pankaj Gupta, Khushbu Saxena, Vivek Kulkarni, Thomas Runkler, and Hinrich Schütze. TopicBERT for energy efficient document classification. In Trevor Cohn, Yulan He, and Yang Liu (eds.), *Findings of the Association for Computational Linguistics: EMNLP 2020*, pp. 1682–1690, Online, November 2020a. Association for Computational Linguistics. doi: 10.18653/v1/2020.findings-emnlp.152. URL <https://aclanthology.org/2020.findings-emnlp.152/>.

541

542

543

544

545

546 Yatin Chaudhary, Pankaj Gupta, Khushbu Saxena, Vivek Kulkarni, Thomas Runkler, and Hinrich Schütze. Topicbert for energy efficient document classification. *Association for Computational Linguistics*, 2020b.

547

548

549

550 Stanley F Chen and Joshua Goodman. An empirical study of smoothing techniques for language modeling. *Computer Speech & Language*, 13(4):359–394, 1999.

551

552

553 Huaqing Cheng, Shengquan Liu, Weiwei Sun, and Qi Sun. A neural topic modeling study integrating sbert and data augmentation. *Applied Sciences*, 13(7):4595, 2023.

554

555 Hans Christian, Mikhael Pramodana Agus, and Derwin Suhartono. Single document automatic text summarization using term frequency-inverse document frequency (tf-idf). *ComTech: Computer, Mathematics and Engineering Applications*, 7(4):285–294, 2016.

556

557

558

559 Benjamin Clavié, Akshita Gheewala, Paul Britton, Marc Alphonsus, Rym Laabiyad, and Francesco Piccoli. Legalmfit: Efficient short legal text classification with lstm language model pre-training. *Association for Computational Linguistics*, 2021.

560

561

562 Şeref Kerem Çorbacıoğlu and Gökhan Aksel. Receiver operating characteristic curve analysis in diagnostic accuracy studies: A guide to interpreting the area under the curve value. *Turkish Journal of Emergency Medicine*, 23(4):195, 2023.

563

564

565

566 Tri Dao, Dan Fu, Stefano Ermon, Atri Rudra, and Christopher Ré. Flashattention: Fast and memory-efficient exact attention with io-awareness. *Advances in neural information processing systems*, 35: 16344–16359, 2022.

567

568

569 Yair Davidson and Nadav Dym. On the holder stability of multiset and graph neural networks. *International Conference on Learning Representations paper*, 2024.

570

571

572 Jacob Devlin, Ming-Wei Chang, Kenton Lee, and Kristina Toutanova. Bert: Pre-training of deep bidirectional transformers for language understanding. In *Proceedings of the 2019 conference of the North American chapter of the association for computational linguistics: human language technologies, volume 1 (long and short papers)*, pp. 4171–4186, 2019.

573

574

575

576 Kaize Ding, Jianling Wang, Jundong Li, Dingcheng Li, and Huan Liu. Be more with less: Hypergraph attention networks for inductive text classification. *Association for Computational Linguistics*, 2020.

577

578

579 Lukas Galke, Andor Diera, Bao Xin Lin, Bhakti Khera, Tim Meuser, Tushar Singhal, Fabian Karl, and Ansgar Scherp. Are we really making much progress in text classification? a comparative review. *Computational Linguistics*, 48(1):4038–4051, 2022.

580

581

582

583 Sander Greenland, Stephen J Senn, Kenneth J Rothman, John B Carlin, Charles Poole, Steven N Goodman, and Douglas G Altman. Statistical tests, p values, confidence intervals, and power: a guide to misinterpretations. *European journal of epidemiology*, 31(4):337–350, 2016.

584

585

586

587 Syed Mustafa Haider Rizvi, Ramsha Imran, and Arif Mahmood. Text classification using graph convolutional networks: A comprehensive survey. *ACM Computing Surveys*, 2025.

588

589

590 David Heckerman. A tutorial on learning with bayesian networks. *Learning in graphical models*, pp. 301–354, 1998.

591

592 Saman Jamshidi, Mahin Mohammadi, Saeed Bagheri, Hamid Esmaeili Najafabadi, Alireza Rezvanian, Mehdi Gheisari, Mustafa Ghaderzadeh, Amir Shahab Shahabi, and Zongda Wu. Effective text classification using bert, mtm lstm, and dt. *Data & Knowledge Engineering*, 151:102306, 2024.

593

594 TianTian Jiang and ZhanGuo Wang. Text classification using bigru with directional self-attention. In  
 595 *2022 11th International Conference of Information and Communication Technology (ICTech)*), pp.  
 596 394–397. IEEE, 2022.

597

598 Simon A Lee, Anthony Wu, and Jeffrey N Chiang. Clinical modernbert: An efficient and long context  
 599 encoder for biomedical text. *Hugging Face*, 2025.

600 Bofang Li, Zhe Zhao, Tao Liu, Puwei Wang, and Xiaoyong Du. Weighted neural bag-of-n-grams  
 601 model: New baselines for text classification. In *Proceedings of COLING 2016, the 26th Interna-*  
 602 *tional Conference on Computational Linguistics: Technical Papers*, pp. 1591–1600, 2016.

603

604 Xi Li and Lili Jia. English text topic classification using bert-based model. *Journal of Computational*  
 605 *Methods in Sciences and Engineering*, pp. 14727978251321982, 2025.

606 Yuxiao Lin, Yuxian Meng, Xiaofei Sun, Qinghong Han, Kun Kuang, Jiwei Li, and Fei Wu. Bert-  
 607 gcn: Transductive text classification by combining gcn and bert. *Association for Computational*  
 608 *Linguistics*, 2021.

609

610 Boting Liu, Weili Guan, Changjin Yang, Zhijie Fang, and Zhiheng Lu. Transformer and graph  
 611 convolutional network for text classification. *International Journal of Computational Intelligence*  
 612 *Systems*, 16(1):161, 2023.

613

614 Qiwen Liu, Tianjian Chen, Jing Cai, and Dianhai Yu. Enlister: baidu’s recommender system for  
 615 the biggest chinese q&a website. In *Proceedings of the sixth ACM conference on Recommender*  
 616 *systems*, pp. 285–288, 2012.

617

618 Zeping Luo, Shiyu Wu, Cindy Weng, Mo Zhou, and Rong Ge. Understanding the robustness of self-  
 619 supervised learning through topic modeling. *International conference on learning representations*,  
 620 2022.

621

622 Mihai Masala, Stefan Ruseti, and Mihai Dascalu. Robert—a romanian bert model. In *Proceedings of*  
 623 *the 28th International Conference on Computational Linguistics*, pp. 6626–6637, 2020.

624

625 Neethu Elizabeth Michael, Ramesh C Bansal, Ali Ahmed Adam Ismail, A Elnady, and Shazia Hasan.  
 626 A cohesive structure of bi-directional long-short-term memory (bilstm)-gru for predicting hourly  
 627 solar radiation. *Renewable Energy*, 222:119943, 2024.

628

629 Farhad Mortezapour Shiri, Thinagaran Perumal, Norwati Mustapha, and Raihani Mohamed. A  
 630 comprehensive overview and comparative analysis on deep learning models: Cnn, rnn, lstm, gru.  
 631 *Journal on Artificial Intelligence 2024 Vol. 6 Issue 1 Pages 301-360*, pp. 2305, 2023.

632

633 Alessandro Moschitti and Roberto Basili. Complex linguistic features for text classification: A  
 634 comprehensive study. In *European conference on information retrieval*, pp. 181–196. Springer,  
 635 2004.

636

637 Fatma Najar and Nizar Bouguila. Smoothed generalized dirichlet: A novel count-data model for  
 638 detecting emotional states. *IEEE Transactions on Artificial Intelligence*, 3(5):685–698, 2021.

639

640 Fatma Najar and Nizar Bouguila. Emotion recognition: A smoothed dirichlet multinomial solution.  
 641 *Engineering Applications of Artificial Intelligence*, 107:104542, 2022.

642

643 Ramesh Nallapati, Thomas Minka, Hugo Zaragoza, and Stephen Robertson. The smoothed-dirichlet  
 644 distribution: Explaining kl-divergence based ranking in information retrieval. *def*, 2:32, 2007.

645

646 Jinseok Nam, Eneldo Loza Mencía, Hyunwoo J Kim, and Johannes Fürnkranz. Maximizing subset ac-  
 647 curacy with recurrent neural networks in multi-label classification. *Advances in neural information*  
 648 *processing systems*, 30, 2017.

649

650 Akinlolu Oluwabusayo Ojo and Nizar Bouguila. A topic modeling and image classification frame-  
 651 work: The generalized dirichlet variational autoencoder. *Pattern Recognition*, 146:110037, 2024.

652

653 Akinlolu Oluwabusayo Ojo, Fatma Najar, Nuha Zamzami, Hanen T Himdi, and Nizar Bouguila.  
 654 Smoothdectector: A smoothed dirichlet multimodal approach for combating fake news on social  
 655 media. *IEEE Access*, 13:39289–39305, 2025.

648 Yinhua Piao, Sangseon Lee, Dohoon Lee, and Sun Kim. Sparse structure learning via graph neural  
 649 networks for inductive document classification. In *Proceedings of the AAAI conference on artificial*  
 650 *intelligence*, volume 36, pp. 11165–11173, 2022.

651

652 Wisam A Qader, Musa M Ameen, and Bilal I Ahmed. An overview of bag of words; importance,  
 653 implementation, applications, and challenges. In *2019 international engineering conference (IEC)*,  
 654 pp. 200–204. IEEE, 2019.

655

656 Rukhma Qasim, Waqas Haider Bangyal, Mohammed A Alqarni, and Abdulwahab Ali Almazroi.  
 657 A fine-tuned bert-based transfer learning approach for text classification. *Journal of healthcare*  
 658 *engineering*, 2022(1):3498123, 2022.

659

660 Mirco Ravanelli, Philemon Brakel, Maurizio Omologo, and Yoshua Bengio. Light gated recurrent  
 661 units for speech recognition. *IEEE Transactions on Emerging Topics in Computational Intelligence*,  
 662 2(2):92–102, 2018.

663

664 Victor Sanh, Lysandre Debut, Julien Chaumond, and Thomas Wolf. Distilbert, a distilled version of  
 665 bert: smaller, faster, cheaper and lighter. *Hugging Face*, 2019.

666

667 Chi Sun, Xipeng Qiu, Yige Xu, and Xuanjing Huang. How to fine-tune bert for text classification? In  
 668 *China national conference on Chinese computational linguistics*, pp. 194–206. Springer, 2019a.

669

670 Xia Sun, Yi Gao, Richard Sutcliffe, Shou-Xi Guo, Xin Wang, and Jun Feng. Word representation  
 671 learning based on bidirectional grus with drop loss for sentiment classification. *IEEE Transactions*  
 672 *on Systems, Man, and Cybernetics: Systems*, 51(7):4532–4542, 2019b.

673

674 Zoubir Talai and Nada Kherici. Compact cnn-based architecture for text classification and sentiment  
 675 analysis. *Revue de l'Information Scientifique et Technique*, 27(2):50–55, 2023.

676

677 Ashish Vaswani, Noam Shazeer, Niki Parmar, Jakob Uszkoreit, Llion Jones, Aidan N Gomez, Łukasz  
 678 Kaiser, and Illia Polosukhin. Attention is all you need. *Advances in neural information processing*  
 679 *systems*, 30, 2017.

680

681 Daniel Voskergian, Rashid Jayousi, and Malik Yousef. Topic selection for text classification using  
 682 ensemble topic modeling with grouping, scoring, and modeling approach. *Scientific Reports*, 14  
 683 (1):23516, 2024.

684

685 Congcong Wang, Paul Nulty, and David Lillis. A comparative study on word embeddings in deep  
 686 learning for text classification. In *Proceedings of the 4th international conference on natural*  
 687 *language processing and information retrieval*, pp. 37–46, 2020a.

688

689 Dongsheng Wang, Dandan Guo, He Zhao, Huangjie Zheng, Korawat Tanwisuth, Bo Chen, and  
 690 Mingyuan Zhou. Representing mixtures of word embeddings with mixtures of topic embeddings.  
 691 *International conference on learning representations*, 2022.

692

693 Shiyu Wang, Gang Zhou, Jicang Lu, Jing Chen, and Ningbo Huang. Pre-trained semantic inter-  
 694 action based inductive graph neural networks for text classification. In *Proceedings of the 31st*  
 695 *International Conference on Computational Linguistics*, pp. 812–827, 2025.

696

697 Yizhao Wang, Chenxi Wang, Jieyu Zhan, Wenjun Ma, and Yuncheng Jiang. Text fcg: Fusing  
 698 contextual information via graph learning for text classification. *Expert Systems with Applications*,  
 699 219:119658, 2023.

700

701 Ziniu Wang, Zhilin Huang, and Jianling Gao. Chinese text classification method based on bert  
 702 word embedding. In *Proceedings of the 2020 5th International Conference on Mathematics and*  
 703 *Artificial Intelligence*, pp. 66–71, 2020b.

704

705 Benjamin Warner, Antoine Chaffin, Benjamin Clavié, Orion Weller, Oskar Hallström, Said  
 706 Taghadouini, Alexis Gallagher, Raja Biswas, Faisal Ladhak, Tom Aarsen, et al. Smarter, bet-  
 707 ter, faster, longer: A modern bidirectional encoder for fast, memory efficient, and long context  
 708 finetuning and inference. *Association for Computational Linguistics: Anonymous submission*,  
 709 2024.

702 Xiaobao Wu, Thong Nguyen, and Anh Tuan Luu. A survey on neural topic models: methods,  
703 applications, and challenges. *Artificial Intelligence Review*, 57(2):18, 2024.  
704

705 Shi-Tao Yeh et al. Using trapezoidal rule for the area under a curve calculation. *Proceedings of the*  
706 *27th Annual SAS® User Group International (SUGI'02)*, 4:1, 2002.  
707

708 Kaiyu Yue, Ming Sun, Yuchen Yuan, Feng Zhou, Errui Ding, and Fuxin Xu. Compact generalized  
709 non-local network. *Advances in neural information processing systems*, 31, 2018.  
710

711 Xiang Zhang, Junbo Zhao, and Yann LeCun. Character-level convolutional networks for text  
712 classification. *Advances in neural information processing systems*, 28, 2015.  
713

714 Yufeng Zhang, Xueli Yu, Zeyu Cui, Shu Wu, Zhongzhen Wen, and Liang Wang. Every document owns  
715 its structure: Inductive text classification via graph neural networks. *Association for Computational*  
716 *Linguistics*, 2020.  
717

718

719

720

721

722

723

724

725

726

727

728

729

730

731

732

733

734

735

736

737

738

739

740

741

742

743

744

745

746

747

748

749

750

751

752

753

754

755

756 A APPENDIX  
757758 B PSEUDOCODE FOR SD-MoBERT GENERATIVE PROCESS  
759

760 In this section, we present the high-level algorithmic steps of SD-MoBERT’s generative process.  
 761 Algorithm 1 outlines how each document is first encoded via a bag-of-words topic model and a ModernBERT backbone, then dynamically fused through a smoothed-Dirichlet co-attention mechanism,  
 762 and finally passed through a classification head. By iterating thematic nuances for the smoothed-  
 763 Dirichlet prior and jointly optimizing the transformer and topic parameters, SD-MoBERT learns to  
 764 leverage both topical and contextual information in a unified training loop.  
 765

767 **Algorithm 1** Generative process for SD-MoBERT

```

768 1: Data:
769 2:    $M$ : document tokens  $\{w_1, \dots, w_N\}$ 
770 3:    $y$ : true label
771 4: Parameters:
772 5:   Transformer weights (ModernBERT)
773 6:   Topic MLP weights  $\{W^{(i)}, b^{(i)}\}$ ,
774 7:      $W_\mu, b_\mu, W_{\log \sigma}, b_{\log \sigma}, W_\alpha, b_\alpha$ 
775 8:   Fusion weights  $W_t, b_t, W_c, b_c, b_0, W_1, b_1, W_2, b_2$ 
776 9: Result:
777 10:  Logits  $\mathbf{o}$ , loss  $\mathcal{L}_{\text{total}}$ 
778 11:  Initialize all parameters
779 12: while not converged do
780 13:  // 1. Prepare Inputs
781 14:   $\mathbf{X} \leftarrow \text{BoW}(M)$  ▷ size  $V$ 
782 15:   $\{t_1, \dots, t_T\} \leftarrow \text{Tokenize}(M)$  ▷  $T \leq 8192$ 
783 16:   $\mathbf{E} \leftarrow \text{ModernBERT}(\{t_i\})$  ▷ size  $T \times D$ 
784 17:   $\mathbf{h}_{\text{CLS}} \leftarrow \mathbf{E}[0]$  ▷  $D$ -dim
785 18:
786 19:  // 2. Neural Topic Model Inference ▷ size  $H$ 
787 20:   $\boldsymbol{\pi} \leftarrow \text{MLP}(\mathbf{X})$ 
788 21:   $\boldsymbol{\mu} \leftarrow W_\mu \boldsymbol{\pi} + b_\mu$ 
789 22:   $\log \boldsymbol{\sigma} \leftarrow W_{\log \sigma} \boldsymbol{\pi} + b_{\log \sigma}$ 
790 23:   $\boldsymbol{\alpha} \leftarrow W_\alpha \boldsymbol{\pi} + b_\alpha$ 
791 24:   $\epsilon \sim \mathcal{N}(0, I)$ 
792 25:   $\boldsymbol{\alpha}_{SD} \leftarrow \boldsymbol{\alpha} + \boldsymbol{\mu} + \epsilon \odot \exp(\log \boldsymbol{\sigma})$ 
793 26:   $\mathbf{Z}_{SD} \leftarrow \text{softmax}(\boldsymbol{\alpha}_{SD})$ 
794 27:
795 28:  // 3. Co-Attention Fusion
796 29:   $\mathbf{Z}_{SD}^t \leftarrow \text{GELU}(W_t \mathbf{Z}_{SD} + b_t)$ 
797 30:   $\mathbf{Z}_{CLS} \leftarrow \text{GELU}(W_c \mathbf{h}_{\text{CLS}} + b_c)$ 
798 31:   $S \leftarrow \langle \mathbf{Z}_{SD}^t, \mathbf{Z}_{CLS} \rangle + b_0$ 
799 32:   $\mathbf{Z}_{\text{att}} \leftarrow \sigma(S)$ 
800 33:   $\mathbf{Z}_{\text{fused}} \leftarrow \mathbf{Z}_{\text{att}} \mathbf{Z}_{SD}^t + (1 - \mathbf{Z}_{\text{att}}) \mathbf{Z}_{CLS}$ 
801 34:   $\mathbf{Z} \leftarrow \tanh(\mathbf{Z}_{\text{fused}})$ 
802 35:
803 36:  // 4. Classification Head
804 37:   $\mathbf{h}_1 \leftarrow \text{GELU}(W_1 \mathbf{Z} + b_1)$ 
805 38:   $\mathbf{o} \leftarrow W_2 \mathbf{h}_1 + b_2$ 
806 39:
807 40:  // 5. Loss
808 41:   $\mathcal{L}_{\text{CE}} \leftarrow \text{CrossEntropy}(\mathbf{o}, y)$ 
809 42:   $\mathcal{L}_{\text{KL}} \leftarrow \text{KL\_Dirichlet}(\tilde{\boldsymbol{\alpha}} \parallel \alpha_0 \mathbf{1})$ 
810 43:   $\mathcal{L}_{\text{total}} \leftarrow \mathcal{L}_{\text{CE}} + \lambda \mathcal{L}_{\text{KL}}$ 
811 44:  Update parameters via optimizer
812 45: end while

```

810 B.1 SMOOTHED DIRICHLET THEMATIC LOSS: KULLBACK-LEIBLER DIVERGENCE (KL)  
811812 Below we extend the standard Dirichlet-to-Dirichlet KL proof to the case where both distributions  
813 include an additive smoothing parameter  $\varepsilon > 0$ . In essence, if  
814

815 
$$P = \text{Dir}(\boldsymbol{\alpha} + \varepsilon \mathbf{1}), \quad Q = \text{Dir}(\boldsymbol{\beta} + \varepsilon \mathbf{1}), \quad (10)$$
  
816

817 then the KL divergence  $\text{KL}[P\|Q]$  takes exactly the same closed-form as for the unsmoothed case,  
818 with each  $\alpha_i$  and  $\beta_i$  replaced by  $\alpha_i + \varepsilon$  and  $\beta_i + \varepsilon$ , respectively.  
819820 The Dirichlet density with smoothing  $\varepsilon$  is defined for  $\mathbf{X} \in \Delta^{K-1}$  by  
821

822 
$$p(\mathbf{X} \mid \boldsymbol{\alpha}, \varepsilon) = \frac{1}{B(\boldsymbol{\alpha} + \varepsilon \mathbf{1})} \prod_{i=1}^K X_i^{(\alpha_i + \varepsilon) - 1}, \quad (11)$$
  
823

824 where  
825

826 
$$B(\boldsymbol{\alpha} + \varepsilon) = \frac{\prod_{i=1}^K \Gamma(\alpha_i + \varepsilon)}{\Gamma(\sum_{i=1}^K (\alpha_i + \varepsilon))} \quad (12)$$
  
827

828 is the multivariate Beta function Nallapati et al. (2007). The standard KL divergence between two  
829 densities  $p$  and  $q$  is  
830

831 
$$\text{KL}[P\|Q] = \int p(\mathbf{x}) \log \frac{p(\mathbf{x})}{q(\mathbf{x})} d\mathbf{x} \quad (13)$$
  
832

833 
$$\text{Let } P(\mathbf{x}) = \text{Dir}(\boldsymbol{\alpha} + \varepsilon \mathbf{1}), \quad Q(\mathbf{x}) = \text{Dir}(\boldsymbol{\beta} + \varepsilon \mathbf{1}). \quad (14)$$
  
834

835 Substituting both into the KL definition and bringing out constant terms yields  
836

837 
$$\begin{aligned} \text{KL}[P\|Q] &= \int P(\mathbf{x}) \left[ \log \frac{B(\boldsymbol{\beta} + \varepsilon)}{B(\boldsymbol{\alpha} + \varepsilon)} + \sum_{i=1}^K ((\alpha_i + \varepsilon) - (\beta_i + \varepsilon)) \log x_i \right] d\mathbf{x} \\ &= \log \frac{B(\boldsymbol{\beta} + \varepsilon)}{B(\boldsymbol{\alpha} + \varepsilon)} + \sum_{i=1}^K (\alpha_i - \beta_i) \mathbb{E}_P[\log x_i], \end{aligned} \quad (15)$$
  
838

839 For a smoothed Dirichlet with parameters  $\alpha'_i = \alpha_i + \varepsilon$ , the moment is  
840

841 
$$\mathbb{E}[\log x_i] = \psi(\alpha_i + \varepsilon) - \psi\left(\sum_{j=1}^K (\alpha_j + \varepsilon)\right), \quad (16)$$
  
842

843 where  $\psi$  is the digamma function. Writing the log-ratio of Beta functions in terms of Gamma yields  
844

845 
$$\log \frac{B(\boldsymbol{\beta} + \varepsilon)}{B(\boldsymbol{\alpha} + \varepsilon)} = \sum_{i=1}^K [\log \Gamma(\beta_i + \varepsilon) - \log \Gamma(\alpha_i + \varepsilon)] + \log \Gamma\left(\sum_i \alpha_i + K\varepsilon\right) - \log \Gamma\left(\sum_i \beta_i + K\varepsilon\right) \quad (17)$$
  
846

847 Combining the above parts, the KL divergence between two smoothed Dirichlet distributions is  
848

849 
$$\begin{aligned} \mathcal{L}_{\text{KL}} \implies \text{KL}[\text{Dir}(\boldsymbol{\alpha} + \varepsilon) \parallel \text{Dir}(\boldsymbol{\beta} + \varepsilon)] &= \sum_{i=1}^K [\log \Gamma(\beta_i + \varepsilon) - \log \Gamma(\alpha_i + \varepsilon)] \\ &+ \log \Gamma\left(\sum_{i=1}^K \alpha_i + K\varepsilon\right) - \log \Gamma\left(\sum_{i=1}^K \beta_i + K\varepsilon\right) \\ &+ \sum_{i=1}^K (\alpha_i - \beta_i) [\psi(\alpha_i + \varepsilon) - \psi(\sum_{j=1}^K \alpha_j + K\varepsilon)] \end{aligned} \quad (18)$$
  
850

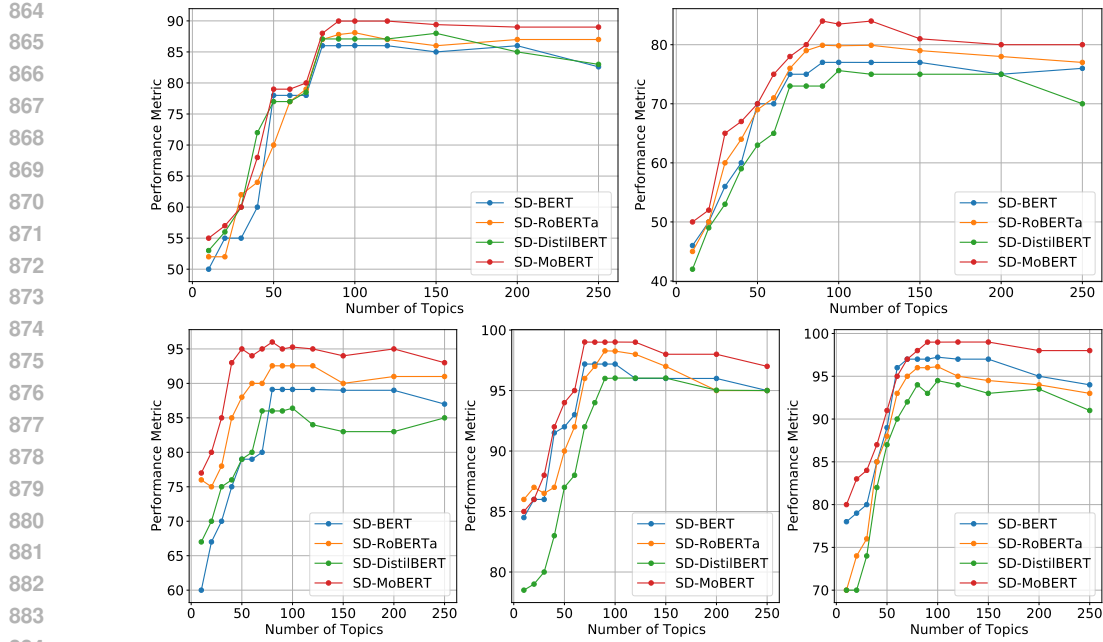


Figure 4: Sensitivity of classification accuracy to the number of latent topics on five data sets. Each subplot corresponds to a different dataset: MR (top left), Ohsuemed (top right), 20NG (bottom left), Reuters R8 (bottom center), and Reuters R52 (bottom right),  $\beta = 0.2$ .

Note that this expression reduces to the standard Dirichlet KL divergence when  $\varepsilon \rightarrow 0$ .

### C EFFECT OF TOPIC NUMBER ON CLASSIFICATION PERFORMANCE

C depicts how the variation in the number of latent topics influences the classification accuracy in five benchmark datasets (MR, Ohsuemed, 20 Newsgroups, R8, and R52) for four smoothed-Dirichlet variants: SD-BERT, SD-RoBERTa, SD-DistilBERT, and SD-MoBERT. In all cases, performance increases when the topic number increases from very low values (10-40), reflecting the transition from an overly coarse to a sufficiently expressive latent representation. Beyond approximately 70-100 topics, gains begin to plateau or even fluctuate slightly, indicating diminishing returns from further topic subdivisions.

On the Movie Review (MR) dataset, SD-MoBERT achieves the highest peak accuracy of roughly 90% at 80 topics, outperforming its counterparts by 2-4%, while all models converge around 86-88% for larger topic numbers. A similar pattern emerges on Ohsuemed: SD-MoBERT reaches about 84% at 90-100 topics, whereas the other transformers level off around 77-80%. In the more fine-grained 20 Newsgroups setting, SD-MoBERT again leads with nearly 96% at 80 topics, compared to 92-93% for SD-RoBERTa and SD-BERT, and slightly lower performance for the DistilBERT variant. For the more specialized Reuters subsets R8 and R52, the advantage of SD-MoBERT is most pronounced. On R8, SD-MoBERT rapidly climbs to over 99% accuracy at 80 topics and sustains this around 98-99% as topics increase. The other models attain roughly 96-98% in the same range, with SD-DistilBERT typically the lowest. On R52, SD-MoBERT surpasses 99% by 100 topics, while SD-RoBERTa and SD-BERT stabilize around 95-97%, and SD-DistilBERT around 91-94%.

In general, these plots demonstrate that integrating ModernBERT with a smoothed Dirichlet topic prior (SD-MoBERT) consistently yields better classification performance, especially once the latent dimensionality is sufficiently large (70 to 100 topics), and that beyond this range, additional topics confer minimal benefit across various text classification scenarios.

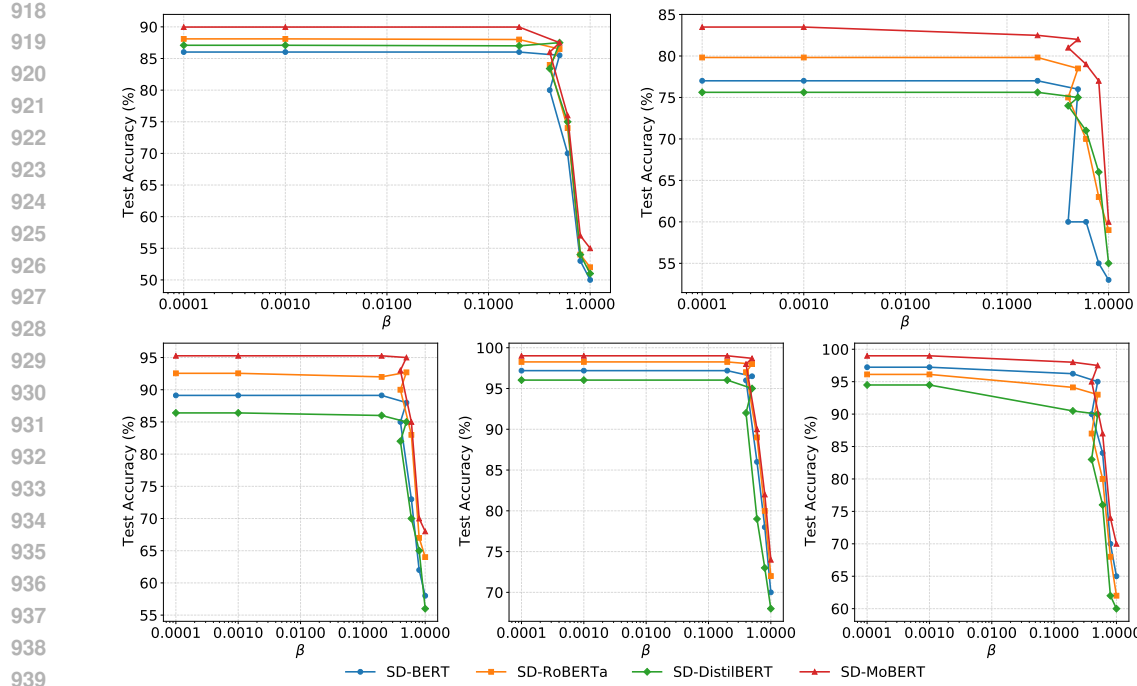


Figure 5: Sensitivity of classification accuracy to the regularization weight  $\beta$  across five benchmarks. Each subplot corresponds to a different dataset: MR (top left), Ohsumed (top right), 20NG (bottom left), Reuters R8 (bottom center), and Reuters R52 (bottom right),  $K = 100$ .

## D EFFECT OF THE KL-WEIGHT FACTOR ON CLASSIFICATION PERFORMANCE

Figure 5 depicts the test-accuracy plots to visualize how the balance between cross-entropy loss and the KL divergence (controlled by the regularization coefficient  $\beta$  in  $\mathcal{L} = \mathcal{L}_{\text{CE}} + \beta \mathcal{L}_{\text{KL}}$ ) affects classification accuracy on five benchmark corpora (MR, Ohsumed, 20NG, R8 and R52).

Across the five benchmarks, we observe the following consistent pattern: when  $\beta$  is large ( $\beta \geq 0.6$ ), the models under-emphasize the cross-entropy term and suffer in accuracy. For example, on the MR, all four methods plateau around 70-80 % at  $\beta \geq 0.6$ . As  $\beta$  decreases into the range  $[0.4, 0.2]$ , the accuracy rises, indicating that the KL regularization has been sufficiently relaxed to allow the classifier to leverage discriminative features while still benefiting from topic-based smoothing. In particular,  $\beta = 0.2$  yields near-peak performance for every dataset. SD-BERT achieves 86.02 % on MR and 89.12 % on 20NG, SD-RoBERTa reaches 88.10 % and 92.55 %, SD-DistilBERT attains 87.09 % and 86.40 %, and SD-MoBERT tops out at 89.97 % and 95.27 %, respectively—while further reductions of  $\beta$  below 0.2 produce only marginal gains or slight degradations.

On the Ohsumed, R8, and R52 corpora a similar “elbow” appears at  $\beta = 0.2$ : performance rises from the mid-70s to the high-70s or low-80s as  $\beta$  falls from 0.6 to 0.2, then asymptotes or even dips slightly for  $\beta < 0.2$ . This behaviour confirms that  $\beta = 0.2$  achieves the optimal trade-off between enforcing the consistency of the topic model (via  $\mathcal{L}_{\text{KL}}$ ) and preserving classification accuracy (via  $\mathcal{L}_{\text{CE}}$ ) across all settings. We therefore fix  $\beta = 0.2$  in subsequent experiments, as it uniformly delivers near-best or best accuracy with robust stability across data sets and model backbones.

972    **E HYPOTHESIS TESTING: STATISTICAL COMPARISON OF SD-MoBERT AND**  
 973    **PASIG-S**  
 974

975    Table 3 summarizes the F1 mean, variance, standard deviation ( $S$ ), 95% confidence intervals (CI), and  
 976    two-sided p-values for SD-MoBERT versus the best baseline (PaSIG-S) across the five benchmarks.  
 977

978    We compute each 95% confidence interval using Greenland et al. (2016)

$$979 \quad \text{CI} = \mu \pm z^* \frac{s}{\sqrt{n}}, \quad z^* = 1.96, \quad (19)$$

981    where  $n$  is the number of evaluation runs. For example, on the MR dataset with  $\mu = 88.13$ ,  
 982     $S = 0.029$ , and 30 trials, the resulting interval is [88.120 - 88.140].  
 983

984    To test whether SD-MoBERT’s mean F1 differs from PaSIG-S, we formulate

$$985 \quad H_0: \mu_{\text{SD-MoBERT}} = \mu_{\text{PaSIG-S}} \quad \text{vs.} \quad H_1: \mu_{\text{SD-MoBERT}} \neq \mu_{\text{PaSIG-S}} \quad (20)$$

987    We calculate the two-sided p-value as Greenland et al. (2016)

$$988 \quad p = 2(1 - \text{CDF}(|t|, df)), \quad df = n - 1, \quad (21)$$

990    where

$$991 \quad \text{CDF}(|t|, df) = \int_{-\infty}^{|t|} f(t, df) dt, \quad (22)$$

993    and the Student’s  $t$ -distribution PDF is

$$995 \quad f(t, df) = \frac{\Gamma(\frac{df+1}{2})}{\sqrt{df\pi}\Gamma(\frac{df}{2})} \left(1 + \frac{t^2}{df}\right)^{-\frac{df+1}{2}}. \quad (23)$$

997    where  $df = n - 1$  denotes the degree of freedom and  $\Gamma$  represents the Gamma function.

999    All five datasets yield  $p < 0.05$ , thus, we reject the NULL hypothesis  $H_0$  and accept the alternative  
 1000    hypothesis  $H_1$ . The extremely small p-values (e.g.  $2.38 \times 10^{-47}$  on MR) and tight confidence intervals  
 1001    demonstrate that SD-MoBERT’s improvements over PaSIG-S are both statistically significant and  
 1002    consistently observed.

1004    **F EFFICIENCY ANALYSIS: TIME COMPLEXITY AND RUNTIME COST**  
 1005

1006    Table 4 compares six transformer-based classifiers in terms of their time complexity, approximate  
 1007    floating-point operations per token (FLOPs), and measured CPU inference time on a single Reuters  
 1008    R8 document. All experiments are conducted on a 12th Gen Intel(R) Core(TM) i7-12700K processor  
 1009    (3.60 GHz), 64GB RAM, and a 64-bit operating system. The baseline BERT and its long-context  
 1010    variant MoBERT both exhibit the familiar  $\mathcal{O}(b \cdot L \cdot T^2 \cdot D)$  complexity, where  $b$  denotes the batch  
 1011    size,  $L$  the number of transformer layers,  $T$  the sequence length, and  $D$  the hidden dimension. BERT  
 1012    incurs approximately 148 GFLOPs per token and requires 0.74 ms to process a single R8 document,  
 1013    whereas MoBERT’s optimizations reduce this to 118 GFLOPs and 0.59 ms.

1014    Incorporating the smoothed-Dirichlet topic model adds an  $\mathcal{O}(b(V \cdot H + H \cdot K))$  term (with vo-  
 1015    cabulary size  $V$ , topic-MLP hidden size  $H$ , and  $K$  topics). Thus SD-BERT’s complexity becomes  
 1016     $\mathcal{O}(b(L T^2 D + V H + H K))$ , raising FLOPs to 158 GFLOPs and inference time to 0.79 ms. SD-  
 1017    RoBERTa, which uses a larger embedding dimension  $D_{\text{large}}$ , further increases cost to 220 GFLOPs  
 1018    and 1.10 ms. DistilBERT’s lighter backbone ( $L' < L$ ) yields the fastest pure transformer variant:  
 1019    SD-DistilBERT achieves only 84 GFLOPs and 0.42 ms despite the same topic-model overhead.  
 1020    Finally, SD-MoBERT combines ModernBERT’s quantization advantages with a small co-attention  
 1021    fusion ( $\mathcal{O}(b(D' H'))$ ), resulting in  $\mathcal{O}(b(L T^2 D + V H + H K + D' H'))$ , 126 GFLOPs, and 0.63  
 1022    ms.  $D'$  denotes the fusion layer output dimensionality,  $D_{\text{large}}$  is the larger embedding dimension in  
 1023    RoBERTa-base, and  $H'$  is the hidden layer size in the classification head.

1024    Overall, MoBERT and SD-MoBERT strike the best balance between high capacity and low la-  
 1025    tency, while SD-DistilBERT offers the most lightweight option when computational resources are  
 constrained.

1026 Table 4: Comparison of time complexity, per-token FLOPs, and CPU inference latency on the Reuters  
 1027 R8 dataset (single document) for BERT, MoBERT, and their smoothed-Dirichlet variants.  
 1028

1029 1030 Model	1031 Time complexity	1032 FLOPs	1033 CPU Time (ms)
1031 BERT	$\mathcal{O}(b \cdot L \cdot T^2 \cdot D)$	148 GFLOPs	0.74
1032 MoBERT	$\mathcal{O}(b \cdot L \cdot T^2 \cdot D)$	118 GFLOPs	0.59
1033 SD-BERT	$\mathcal{O}(b \cdot (L \cdot T^2 \cdot D + V \cdot H + H \cdot K))$	158 GFLOPs	0.79
1034 SD-RoBERTa	$\mathcal{O}(b \cdot (L \cdot T^2 \cdot D_{large} + V \cdot H + H \cdot K))$	220 GFLOPs	1.1
1035 SD-DistilBERT	$\mathcal{O}(b \cdot (L' \cdot T^2 \cdot D + V \cdot H + H \cdot K))$	84 GFLOPs	0.42
1036 SD-MoBERT	$\mathcal{O}(b \cdot (L \cdot T^2 \cdot D + V \cdot H + H \cdot K + D' \cdot H'))$	126 GFLOPs	0.63

1041  
 1042 **Listing 1** Smoothed-Dirichlet MLP forward function; see SMDIRICHLET class below.  
 1043

```

 1045 1   def forward(self, input_bows):
 1046 2     # Run BOW through MLP
 1047 3     pi = self.mlp(input_bows)
 1048 4
 1049 5     # Use this to get rho1, log_rho2 for Dirichlet
 1050 6     rho1 = self.rho1(pi)
 1051 7     logrho2 = self.rho2(pi)
 1052 8     alpha = self.alpha(pi)
 1053 9
 105410    epsilon = torch.normal(0, 1, size=
 105511          input_bows.size()[0], self.num_topics)).to(input_bows.device)
 105612
 105713    sample, alpha_smoothed = self.reparameterize(alpha, rho1, logrho2, epsilon)
 105814
 105915    logits = self.log_softmax(self.dec_projection(sample))
 106016
 106117    kld = self.kld(alpha_smoothed, prior_alpha = torch.tensor(0.01), epsilon=torch.tensor(0.01))
 106218    rec_loss = -1 * torch.sum(logits * input_bows, 1)
 106319    loss_nvdm_lb = torch.mean(rec_loss + kld)
 106420
 106521    return sample, logits, torch.mean(kld), loss_nvdm_lb
 106622
 106723
 106824
 106925
 107026
 107127
 107228
 107329
 107430
 107531
 107632
 107733
 107834
 107935

```

---

1080    **Listing 2** Smoothed-Dirichlet MLP (SMDIRICHLET class)

---

```

1082 1 import torch
1083 2 import torch.nn as nn
1084 3 import torch.nn.functional as F
1085 4
1086 5 class SMDIRICHLET(nn.Module):
1087 6
1088 7     @staticmethod
1089 8     def _param_initializer(module):
1090 9         if isinstance(module, nn.Linear):
109110             nn.init.xavier_normal_(module.weight)
109211
109312         if isinstance(module, nn.Linear) and module.bias is not None:
109413             module.bias.data.zero_()
109514
109615     def __init__(self, vocab_size, num_topics=10, hidden_size=256, hidden_layers=1, nonlinearity=nn.ReLU()):
109716         super().__init__()
109817         self.num_topics = num_topics
109918         self.vocab_size = vocab_size
110019
110120         # First MLP layer compresses from vocab_size to hidden_size
110221         mlp_layers = [nn.Linear(vocab_size, hidden_size), nonlinearity()]
110322         # Remaining layers operate in dimension hidden_size
110423         for _ in range(hidden_layers - 1):
110524             mlp_layers.append(nn.Linear(hidden_size, hidden_size))
110625             mlp_layers.append(nonlinearity())
110726
110827         self.mlp = nn.Sequential(*mlp_layers)
110928         self.mlp.apply(SMDIRICHLET._param_initializer)
111029
111130         # Create linear projections for Dirichlet params (rho1 & rho2)
111231         self.rho1 = nn.Linear(hidden_size, num_topics)
111332         self.rho1.apply(SMDIRICHLET._param_initializer)
111433
111534         # Custom initialization for rho2
111635         self.rho2 = nn.Linear(hidden_size, num_topics)
111736         self.rho2.bias.data.zero_()
111837         self.rho2.weight.data.fill_(0.)
111938
112039         # create linear projection for alpha
112140         self.alpha = nn.Linear(hidden_size, num_topics)
112241         self.alpha.apply(SMDIRICHLET._param_initializer)
112342
112443         self.dec_projection = nn.Linear(num_topics, vocab_size)
112544         self.log_softmax = nn.LogSoftmax(-1)
112645
112746     def reparameterize(self, alpha, rho1, logrho2, eps):
112847         rho2 = torch.exp(logrho2)
112948         #eps = torch.randn_like(std)
113049         alpha_smoothed = alpha + eps * rho2 + rho1
113150
113251         Z_sd = F.softmax(alpha_smoothed, dim=1)
113352
113453         return Z_sd, alpha_smoothed
113554
113655     def kld(self, model_alpha, prior_alpha, epsilon):
113756
113857         model_alpha = torch.max(torch.tensor(0.0001), model_alpha).to(model_alpha.device)
113958         alpha = prior_alpha.expand_as(model_alpha)
114059         sum1 = torch.sum((model_alpha + epsilon - 1) * torch.digamma(model_alpha + epsilon), dim=1)
114160
114261         sum2 = torch.sum((alpha + epsilon - 1) * torch.digamma(alpha + epsilon), dim=1)
114362         kl_loss = torch.mean(sum1 - sum2)
114463
114564         return kl_loss

```

---

1134  
1135  
1136  
1137  
1138  
1139  
1140

---

**Listing 3** Smoothed Dirichlet ModernBERT
 

---

```

1142 1   '''This module contains the SD-ModernBERT model with a co-attention mechanism and dynamic
1143 2
1144 3   import torch
1145 4   import torch.nn as nn
1146 5   from transformers import ModernBertModel
1147 6   from models.smdirichlet import SMDIRICHLET
1148 7
1149 8
1150 9   class TopicBERT(nn.Module):
1151 10      '''This module contains the SD-ModernBERT model with a co-attention mechanism and dynamic
1152 11      def __init__(self, vocab_size, num_labels, alpha=0.9, dropout=0.1):
1153 12          super().__init__()
1154 13          self.encoder = ModernBertModel.from_pretrained('answerdotai/ModernBERT-base')
1155 14          self.smdirichlet = SMDIRICHLET(vocab_size)
1156 15
1157 16          # Co-attention projection layers
1158 17          hidden_size = self.encoder.config.hidden_size
1159 18          topic_dim = self.smdirichlet.num_topics
1160 19          self.co_attn_b = nn.Linear(hidden_size, hidden_size, bias=False)
1161 20          self.co_attn_t = nn.Linear(topic_dim, hidden_size, bias=False)
1162 21          self.attn_bias = nn.Parameter(torch.zeros(1))
1163 22
1164 23          # Combine co-attended representation
1165 24          self.combine_proj = nn.Linear(hidden_size, hidden_size)
1166 25
1167 26          # Classification head
1168 27          self.projection = nn.Sequential(
1169 28              nn.Dropout(dropout),
1170 29              nn.Linear(hidden_size, hidden_size, bias=False),
1171 30              nn.GELU(),
1172 31              nn.Linear(hidden_size, num_labels)
1173 32          )
1174 33          self.projection.apply(TopicBERT._get_init_transformer(self.encoder))
1175 34
1176 35          self.bert_loss = nn.CrossEntropyLoss(reduction='mean')
1177 36
1178 37
1179 38      @staticmethod
1180 39      def _get_init_transformer(transformer):
1181 40          def init_transformer(module):
1182 41              if isinstance(module, (nn.Linear, nn.Embedding)):
1183 42                  module.weight.data.normal_(mean=0.0, std=transformer.config.initializer_range)
1184 43              elif isinstance(module, nn.LayerNorm):
1185 44                  module.bias.data.zero_()
1186 45                  module.weight.data.fill_(1.0)
1187 46              if isinstance(module, nn.Linear) and module.bias is not None:
1188 47                  module.bias.data.zero_()
1189 48
1190 49          return init_transformer

```

---

1182  
1183  
1184  
1185  
1186  
1187

---

1188  
 1189  
 1190  
 1191  
 1192  
 1193  
 1194  
 1195  
 1196  
 1197  
 1198  
 1199  
 1200  
 1201  
 1202  
 1203

---

**Listing 4** Smoothed Dirichlet ModernBERT forward function

---

1204  
 1205 **def** **forward**(**self**, input\_ids, attention\_mask, bows, labels):  
 1206 *# BERT encoding*  
 1207 hiddens\_last = **self**.encoder(input\_ids, attention\_mask=attention\_mask)[0]  
 1208 embs = hiddens\_last[:, 0, :] *# [CLS] token embeddings*  
 1209  
 1210 *# Topic model encoding*  
 1211 h\_tm, \_, kld, loss\_diri = **self**.smdirichlet(bows)  
 1212  
 1213 *# Co-attention*  
 1214 proj\_b = **self**.co\_attn\_b(embs) *# (batch\_size, hidden\_size)*  
 1215 proj\_t = **self**.co\_attn\_t(h\_tm) *# (batch\_size, hidden\_size)*  
 1216 *# Compute affinity and attention weight*  
 1217 scores = torch.sum(proj\_b \* proj\_t, dim=1, keepdim=True) + **self**.attn\_bias *# (batch\_size, 1)*  
 1218 alpha = torch.sigmoid(scores) *# (batch\_size, 1)*  
 1219 *#alpha = self.softmax(scores)*  
 1220 *# Fuse representations*  
 1221 joint = alpha \* proj\_b + (1 - alpha) \* proj\_t  
 1222 co\_emb = torch.tanh(**self**.combine\_proj(joint)) *# (batch\_size, hidden\_size)*  
 1223  
 1224 *# Classification*  
 1225 logits = **self**.projection(co\_emb)  
 1226  
 1227 *# Loss computation*  
 1228 loss\_bert = **self**.bert\_loss(logits, labels.max(1).indices)  
 1229 loss\_total = loss\_bert + kld \* 0.2  
 1230 **return** logits, loss\_total, kld

---

1231  
 1232  
 1233  
 1234  
 1235  
 1236  
 1237  
 1238  
 1239  
 1240  
 1241